

A SOLUTION OF 3D HELMHOLTZ EQUATION FOR BOUNDARY GEOMETRY MODELED BY COONS PATCHES USING THE PARAMETRIC INTEGRAL EQUATION SYSTEM

E. ZIENIUK, K. SZERSZEŃ

University of Białystok
Department of Mathematics and Physics
Institute of Computer Science
Sosnowa 64, 15-887 Białystok, Poland
e-mail: ezeniuk@ii.uwb.edu.pl, kszerszen@ii.uwb.edu.pl

(received April 30, 2005; accepted October 25, 2005)

In this paper, the authors propose an algorithm for numerical solution of the 3D Helmholtz equation using the Parametric Integral Equation System (PIES). The PIES, unlike the traditional Boundary Integral Equation (BIE), is characterized by the fact that the boundary geometry has been considered in its mathematical formalism. Polygonal Coons surfaces have been used to describe the 3D domain. This makes it possible to obtain continuous solutions without any discretization of the 3D domain.

Key words: Helmholtz equation, Boundary Integral Equation (BIE), Parametric Integral Equation System (PIES).

1. Introduction

The numerical solution of the Helmholtz equation is usually obtained by the Finite Element Method (FEM) and the Boundary Element Method (BEM). A common feature of these methods is the necessity of dividing the considered domain into finite (in the case of using the FEM method) or boundary elements (in the case of using the BEM method) [4, 9, 6]. The BEM is a numerical technique for solving the Boundary Integral Equation (BIE) based on Green's equation or on single and double layer potentials [4, 1, 6]. Over the last few years important progress has been made in developing the methods for solving the BIE. The spectral [3, 8], dual MEB [5], Galerkin [3] and many others methods [11, 2, 12, 9] are developed and used for solving the BIE. All of these methods are characterized by the fact that they are directly used for numerical solving of the BIE. As the BIE name suggests, from a mathematical point of view these methods are directly defined by the boundary geometry. This generally requires the simultaneous approximation of the boundary geometry and boundary functions. So if the BEM method has been followed, the dependence of the approximation of the shape of the boundary

geometry from the boundary functions on individual elements in which the boundary is divided. Such dependence does not allow for independence increasing the accuracy of the boundary functions without interference of the boundary shape approximation and *vice versa*.

In our works an analytical modification of the BIE [20, 13] was proposed, in order to achieve the separation of the approximation of the boundary shape from the boundary functions. For this reason a variety of curves [10] from a computer graphic were used for the boundary shape definition. As a result of this modification a new equation, called the Parametric Integral Equation System (PIES), was formulated. The obtained PIES is characterized by the fact that the boundary geometry is considered in its mathematical formalism (in kernels) by implemented curves.

The main advantage of PIES in comparison to the classical BIE is the separation of the simultaneous approximation of the boundary geometry from the approximation of the boundary functions in the process of numerical solving. This approach makes it possible to seek more effective ways for modelling the boundary geometry. The practical polygonal domains are defined by characteristic points – corner points. In the case of domains with smooth curved boundaries we need to define additional intermediate points (between corners points). These points may not be able to identify with the nodes from the classical BEM method for the following two reasons. The first reason is that there are a significant fewer number of control points compared to the BEM, and the second reason is that these points allow modeling of the boundary geometry in a continuous way. This approach leads to the elimination of any traditional discretization, not only the domain itself (like in FEM) but also the domain boundary (like in BEM). The proposed technique of the boundary definition has been tested for two-dimensional Laplace [13] and Helmholtz equations [17, 18].

Recent developments in PIES method are concentrated on the generalization of the idea considered in PIES method for 3D boundary problems. Papers [15, 16] present PIES and its numerical method for solving Laplace equation in 3D domains. In this case it has eliminated the inevitable discretization of geometry in the boundary, introducing continuous description 3D boundary geometry using surface patches: rectangular Coons [15] and smooth Bezier [16], defined with the help of small number of control points.

The main aim of the paper is to provide the application of the linear rectangular Coons surfaces for defining the shapes of the boundary geometry in 3D domains modelled by the Helmholtz equation. The pseudospectral method has been used for numerical solving the PIES. This has allowed to obtain continuous (in polynomial form) solutions on all boundary surface patches.

2. The definition of 3D boundary geometry by Coons surfaces

The proposed technique for the geometry description of 3D domain is based on defining a small number of corner points, which describes independent Coons surfaces in terms of two parametric variables v and w for each patch.

The Coons patch is defined as a rectangle with four corner points $P_1(0, 0)$, $P_2(0, 1)$, $P_3(1, 0)$, $P_4(1, 1)$ and can be expressed in a matrix form that permits simple arithmetic calculations [10]

$$P^{(x)}(v, w) = [1 - v, v] \begin{bmatrix} P_1^{(x)}(0, 0) & P_2^{(x)}(0, 1) \\ P_3^{(x)}(1, 0) & P_4^{(x)}(1, 1) \end{bmatrix} \begin{bmatrix} 1 - w \\ w \end{bmatrix}, \quad (1)$$

where $\mathbf{x} \equiv \{x_1, x_2, x_3\}$, $0 < v < 1$, $0 < w < 1$.

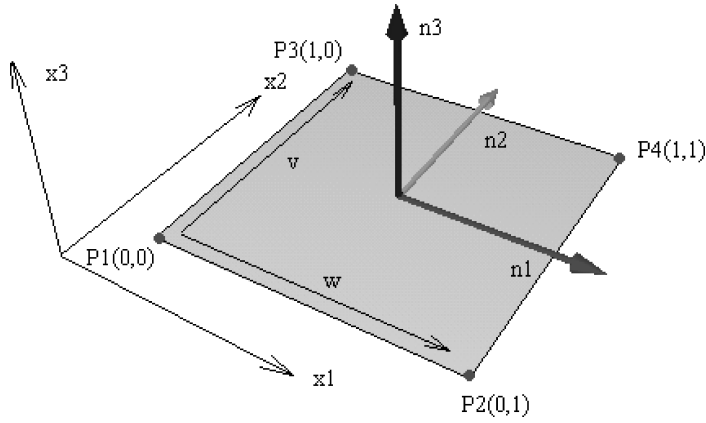


Fig. 1. Notations of parametric coordinate system (v, w) for a Coons surface defined by 4 corner points. The computed normals n_1, n_2, n_3 are directly used in PIES for the overall orientation of individual surfaces.

The Jacobian for every patch is computed by

$$J_j = [A_1^2 + A_2^2 + A_3^2]^{0.5}, \quad (2)$$

where

$$\begin{aligned} A_1 &= \frac{\partial P_j^{(x2)}}{\partial w} \frac{\partial P_j^{(x3)}}{\partial v} - \frac{\partial P_j^{(x2)}}{\partial v} \frac{\partial P_j^{(x3)}}{\partial w}, \\ A_2 &= \frac{\partial P_j^{(x3)}}{\partial w} \frac{\partial P_j^{(x1)}}{\partial v} - \frac{\partial P_j^{(x3)}}{\partial v} \frac{\partial P_j^{(x1)}}{\partial w}, \\ A_3 &= \frac{\partial P_j^{(x1)}}{\partial w} \frac{\partial P_j^{(x2)}}{\partial v} - \frac{\partial P_j^{(x1)}}{\partial v} \frac{\partial P_j^{(x2)}}{\partial w}. \end{aligned} \quad (3)$$

The normal vectors n_1, n_2, n_3 for each Coons surface are obtained by

$$n_m = \frac{A_m}{J_j}, \quad m = 1, 2, 3. \quad (4)$$

We can join several Coons patches together to form a closed surface. This approach creates the tool for effective modelling the given geometry with continuous conditions and reduces the total number of input data. The defined geometry is directly used by the presented PIES algorithm for Helmholtz equation without any discretization of the domain (like in FEM) or the boundary (like in BEM).

3. The PIES method in the case of 3D Helmholtz equation

The Helmholtz equation for the complex valued potential U may be written in the 3D space as [1, 10]

$$\frac{\partial^2 U}{\partial x_1^2} + \frac{\partial^2 U}{\partial x_2^2} + \frac{\partial^2 U}{\partial x_3^2} + k^2 U = 0, \quad \text{for } x \in \Omega, \quad (5)$$

where k is a wave number.

PIES for 3D Helmholtz equations has been obtained in a similar form as 3D Laplace equations [13, 20]. The general formula for these two equations is identical and the difference concerns only the integrand functions \bar{U}_{lj}^* and \bar{P}_{lj}^* (boundary and singular solutions). PIES for 3D Helmholtz equation takes the following form:

$$0.5u_l(v_1, w_1) = \sum_{j=1}^n \int_{v_{j-1}}^{v_j} \int_{w_{j-1}}^{w_j} \left\{ \bar{U}_{lj}^*(v_1, w_1, v, w) p_j(v, w) - \bar{P}_{lj}^*(v_1, w_1, v, w) u_j(v, w) \right\} J_j dv dw, \quad l = 1, 2, 3 \dots n, \quad (6)$$

where $v_{j-1} < v < v_j, w_{j-1} < w < w_j$.

The integrand functions $\bar{U}_{lj}^*(v_1, w_1, v, w)$ and $\bar{P}_{lj}^*(v_1, w_1, v, w)$ provide the system detailed information about the defined 3D geometry of the solved boundary value problem

$$\bar{U}_{lj}^* = \frac{1}{4\pi\eta} e^{-ik\eta} = \frac{1}{4\pi\eta} \{ \cos k\eta - i \sin k\eta \}, \quad \text{and} \quad \bar{P}_{lj}^* = \frac{\partial \bar{U}_{lj}^*}{\partial n}, \quad (7)$$

by connecting with Coons parametric surfaces $P(v, w)$ expressed by the following relations

$$\begin{aligned} \eta(v, w) &= [\eta_1^2 + \eta_2^2 + \eta_3^2]^{0.5}, & \eta_1 &= P_l^{(x_1)}(v_1, w_1) - P_j^{(x_1)}(v, w), \\ \eta_2 &= P_l^{(x_2)}(v_1, w_1) - P_j^{(x_2)}(v, w), & \eta_3 &= P_l^{(x_3)}(v_1, w_1) - P_j^{(x_3)}(v, w). \end{aligned} \quad (8)$$

The Jacobian J_j from (6) for every patch is computed by formula (2).

Kernels $\bar{U}_{lj}^*, \bar{P}_{lj}^*$ can be expressed in a matrix form as

$$\bar{U}_{lj}^* = \begin{bmatrix} U_{11}^* & U_{12}^* \\ U_{21}^* & U_{22}^* \end{bmatrix} = \begin{bmatrix} \text{Re}\{U^*\} & -\text{Im}\{U^*\} \\ \text{Im}\{U^*\} & \text{Re}\{U^*\} \end{bmatrix}, \quad (9)$$

where

$$\begin{aligned} U_{11}^* &= U_{22}^* = \operatorname{Re}\{U^*\} = \frac{1}{4\pi\eta} \cos k\eta, \\ U_{12} &= -\operatorname{Im}\{U^*\} = \frac{1}{4\pi\eta} \sin k\eta, \\ U_{21} &= \operatorname{Im}\{U^*\} = -\frac{1}{4\pi\eta} \sin k\eta \end{aligned}$$

and

$$\overline{P}_{lj}^* = \begin{bmatrix} P_{11}^* & P_{12}^* \\ P_{21}^* & P_{22}^* \end{bmatrix} = \begin{bmatrix} \operatorname{Re}\{P^*\} & -\operatorname{Im}\{P^*\} \\ \operatorname{Im}\{P^*\} & \operatorname{Re}\{P^*\} \end{bmatrix}, \quad (10)$$

$$P_{11}^* = P_{22}^* = \operatorname{Re}\{P^*\} = \frac{\cos k\eta + \eta \sin k\eta}{4\pi\eta^3} \{\eta_1 n_1 + \eta_2 n_2 + \eta_3 n_3\},$$

$$P_{12}^* = -\operatorname{Im}\{P^*\} = -\frac{\eta \cos k\eta - \sin k\eta}{4\pi\eta^3} \{\eta_1 n_1 + \eta_2 n_2 + \eta_3 n_3\},$$

$$P_{21}^* = \operatorname{Im}\{P^*\} = \frac{\eta \cos k\eta - \sin k\eta}{4\pi\eta^3} \{\eta_1 n_1 + \eta_2 n_2 + \eta_3 n_3\}.$$

The normal vectors for each Coons surface in (10) are computed by formula (4).

The polygonal boundary geometry is considered in the kernels (7) of the PIES with the help of rectangular Coons surfaces $P_j(v, w)$, ($l = j$). Coons patches used for building the 3D boundary in the way presented in Fig. 2 (regardless of their size) are defined by four corner points $P_1(0, 0)$, $P_2(0, 1)$, $P_3(1, 0)$, $P_4(1, 1)$.

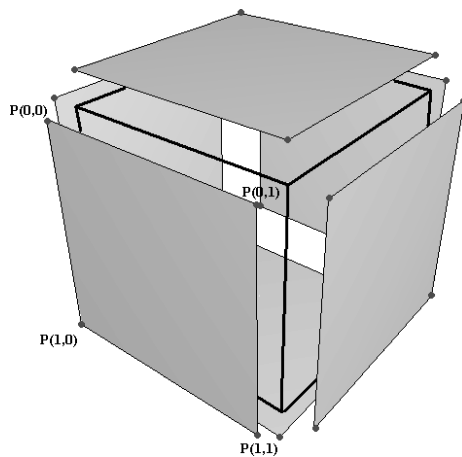


Fig. 2. A cubic domain of any size modelled by 8 corner points. The Coons patch technique uses the setting corner points to construct a numerical model of the surface so that any point on the surface may be obtained in terms of two parameters (v, w) for every patch.

Mathematical description of Coons surface in PIES are expressed in normalized form by formula (1). The presented way of defining 3D boundary in PIES does not require using the traditional boundary elements. In practical case we need to declare only corner points for the domain definition. The number of these points for the domains are identical in shape and independent from their capacity. Such boundary modelling has a big advantage in comparison to element methods, where the capacity of the domain has a crucial affect on the number of its elements.

4. Numerical solution of the PIES

The solution of the PIES is reduced to finding the unknown boundary functions $u_j(v, w)$ or $p_j(v, w)$ defined on individual j Coons surface as the following approximating complex form:

$$p_j(v, w) = \sum_{p=0}^N \sum_{r=0}^M \left\{ u_j^{(pr)} + i v_j^{(pr)} \right\} T_j^{(p)}(v) T_j^{(r)}(w), \quad (11)$$

$$u_j(v, w) = \sum_{p=0}^N \sum_{r=0}^M \left\{ r_j^{(pr)} + i s_j^{(pr)} \right\} T_j^{(p)}(v) T_j^{(r)}(w), \quad (12)$$

where $u_j^{(pr)}$, $v_j^{(pr)}$, $r_j^{(pr)}$, $s_j^{(pr)}$ are the unknown coefficients, $\bar{n} = N \times M$ is the number of coefficients on each Coons surface, $T_j^{(p)}(v)$, $T_j^{(r)}(w)$ are the global base functions – Chebyshev polynomials.

One of these functions $u_j(v, w)$ (or $p_j(v, w)$) depending on the solved boundary problem will be taken the from form of boundary conditions, however the second will be found in the results of the PIES solution.

The insertion (11) and (12) to (6) and using pseudospectral collocation method with collocation points [2] for numerical solving PIES leads to obtain the complete system of linear algebraic equations to determine unknown values of the coefficients $r_j^{(pr)}$, $s_j^{(pr)}$, $u_j^{(pr)}$, $v_j^{(pr)}$ on each segment

$$[H] \{\bar{u}_j\} = [G] \{\bar{p}_j\}, \quad (13)$$

where

$$0.5u_l(v_1, w_1) = \sum_{j=1}^n \sum_{p=0}^N \sum_{r=0}^M \left\{ \left(u_j^{(pr)} + j v_j^{(pr)} \right) \int_{v_{j-1}}^{v_j} \int_{w_{j-1}}^{w_j} \bar{U}_{ij}^*(v_1, w_1, v, w) - \left(r_j^{(pr)} + j s_j^{(pr)} \right) \int_{v_{j-1}}^{v_j} \int_{w_{j-1}}^{w_j} \bar{P}_{ij}^*(v_1, w_1, v, w) \right\} T_j^{(p)}(v) T_j^{(r)}(w) J_j dv dw. \quad (14)$$

Unknown coefficients $u_j^{(k)}, v_j^{(k)}$ or $r_j^{(k)}, s_j^{(k)}$ are solution of algebraic equation system (14). Multiplication coefficients with base functions in (11) and (12) leads to continuous solution on each segment.

5. Solution in the domain

After solving with PIES a solution on the boundary is only obtained. The solution at any point $\mathbf{x} \equiv \{x_1, x_2, x_3\}$ in the domain can then be obtained by integral identity presented below [13]

$$u(\mathbf{x}) = \sum_{j=1}^n \int_{v_{j-1}}^{v_j} \int_{w_{j-1}}^{w_j} \left\{ \widehat{U}_j^*(\mathbf{x}, v, w) p_j(v, w) - \widehat{P}_j^*(\mathbf{x}, v, w) u_j(v, w) \right\} J_j \, dv \, dw, \quad \mathbf{x} \equiv \{x_1, x_2, x_3\}. \quad (15)$$

The information about boundary is included in the kernel functions $\widehat{U}_j^*(\mathbf{x}, v, w)$ and $\widehat{P}_j^*(\mathbf{x}, v, w)$ and presented in the following form the same way as (9) and (10)

$$\begin{aligned} \overline{U}_{lj}^*(\mathbf{x}, v, w) &= \frac{1}{4\pi r} e^{-ikr} = \frac{1}{4\pi r} \{ \cos kr - i \sin kr \}, \quad \text{and} \\ \overline{P}_{lj}^*(\mathbf{x}, v, w) &= \frac{\partial \overline{U}_{lj}^*}{\partial n}, \end{aligned} \quad (16)$$

where

$$r(v, w) = \left[\vec{r}_1^2 + \vec{r}_2^2 + \vec{r}_3^2 \right]^{0.5} \quad (17)$$

and

$$\vec{r}_1 = x_1 - P_j^{(x_1)}(v, w), \quad \vec{r}_2 = x_2 - P_j^{(x_2)}(v, w), \quad \vec{r}_3 = x_3 - P_j^{(x_3)}(v, w). \quad (18)$$

The $P_j^{(x)}(v, w)$ are the same Coons patches used for 3D domain definition.

$$u(\mathbf{x}) = \sum_{j=1}^n \sum_{p=0}^N \sum_{r=0}^M \left\{ \left(u_j^{(pr)} + j v_j^{(pr)} \right) \int_{v_{j-1}}^{v_j} \int_{w_{j-1}}^{w_j} \overline{U}_{ij}^*(\mathbf{x}, v, w) - \left(r_j^{(pr)} + j s_j^{(pr)} \right) \int_{v_{j-1}}^{v_j} \int_{w_{j-1}}^{w_j} \overline{P}_{ij}^*(\mathbf{x}, v, w) \right\} T_j^{(p)}(v) T_j^{(r)}(w) J_j \, dv \, dw. \quad (19)$$

The solution in domain does not require solution on the boundary, only the coefficients $u_j^{(pr)}, v_j^{(pr)}, r_j^{(pr)}, s_j^{(pr)}$ from approximating the sum of $p_j(v, w)$ and $u_j(v, w)$ (11) and $u_j(v, w)$ (12) are used as follows.

6. Results

The practical aspects of the proposed method have been demonstrated by numerical examples. The PIES solution of Helmholtz equations have been analyzed by different 3D polygonal domains and compared with the exact values.

6.1. Example 1

The PIES makes it possible to easily define the boundary geometry. A representation of 3D domain defined with the help of only corner points is specified in Fig. 3.

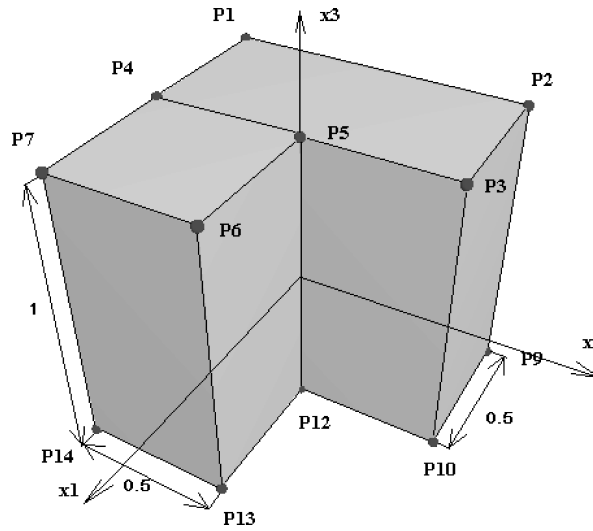


Fig. 3. The boundary geometry definition by Coons surfaces.

The given domain is approximated by 10 linear Coons patches that are described by only 14 corner points P_i ($i = 1 \dots 14$). This geometric model is directly used by PIES in the process of solving the boundary value problem. Alternative element methods (FEM and BEM) require discretizing of the obtained boundary geometry and this considerably raises the cost of computation.

The Dirichlet boundary conditions are given as functions on each Coons surfaces by

$$\begin{aligned} \operatorname{Re} \{U(x_1, x_2, x_3)\} &= \cos(k(x_1 \cos \alpha + x_2 \sin \alpha)) + x_3, \\ \operatorname{Im} \{U(x_1, x_2, x_3)\} &= \sin(k(x_1 \cos \alpha + x_2 \sin \alpha)). \end{aligned} \quad (20)$$

The analytical solution is

$$U(x_1, x_2, x_3) = e^{ik(x_1 \cos \alpha + x_2 \sin \alpha)} + x_3, \quad (21)$$

where $\alpha = (0 \div 90^\circ)$.

The obtained results on cross-section on the boundary (for $k = 1$ and two values of $\alpha - 45^\circ$ and 90°) are graphically presented in Fig. 4.

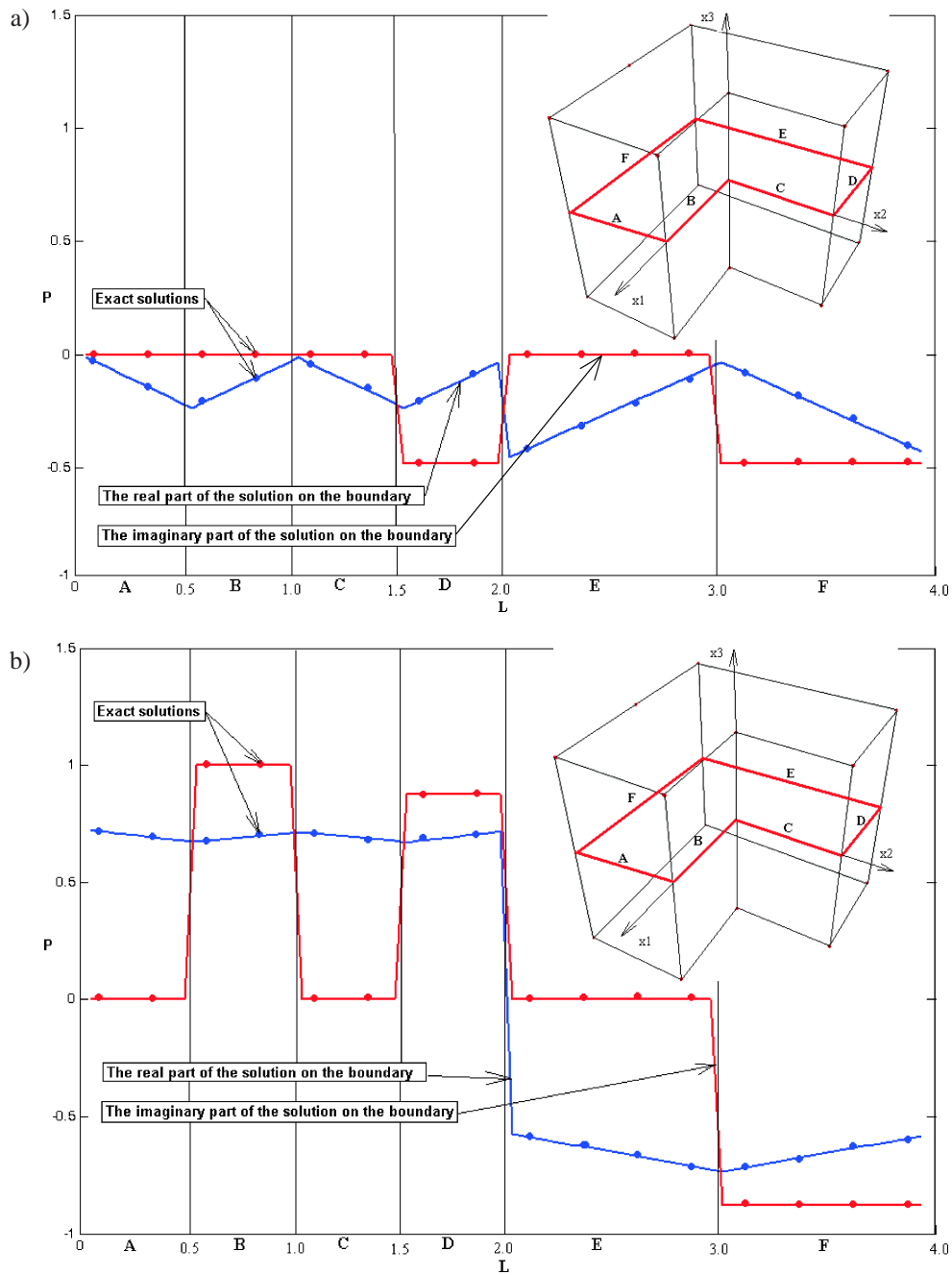


Fig. 4. The study of cross-sectional representation of results on the boundary for two values of α :
 a) $\alpha = 45^\circ$, b) $\alpha = 90^\circ$.

With the help of formula (21) we can obtain analytical solutions for all points on the boundary (marked in Fig. 4)

$$\begin{aligned} \operatorname{Re}\{P(x_1, x_2, x_3)\} &= -\cos \alpha * \sin(k(x_1 \cos \alpha + x_2 \sin \alpha)) * n_1 \\ &\quad + \sin \alpha * \sin(k(x_1 \cos \alpha + x_2 \sin \alpha)) * n_2 + n_3, \\ \operatorname{Im}\{P(x_1, x_2, x_3)\} &= \cos \alpha * \cos(k(x_1 \cos \alpha + x_2 \sin \alpha)) * n_1 \\ &\quad + \sin \alpha * \cos(k(x_1 \cos \alpha + x_2 \sin \alpha)) * n_2. \end{aligned} \quad (22)$$

Based on the result presented in Fig. 4 the solutions on the boundary are close to exact solutions using $\bar{n} = 9$ expressions from the approximating sum (11). In this case we need to solve the system of 90 algebraic equations.

6.2. Example 2

In example 2 we analyze solutions of Helmholtz equation by the PIES for another domain presented in Fig. 5. The domain is described by 17 corner points that define 12 Coons surfaces. The Dirichlet boundary conditions are adopted in the form described by (20).

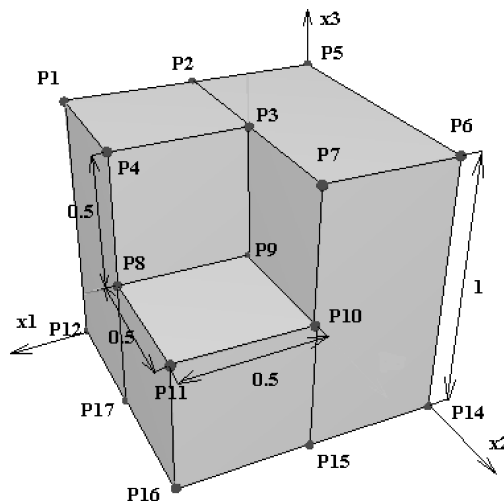


Fig. 5. Graphic representation of the 3D geometry is defined by 17 corner points and 12 Coons surfaces.

By using the PIES i.e. (12), we obtain an approximate solution on the boundary. After obtaining the solution on the boundary and making use of the integral identity (16) we obtain an approximate solution $\hat{u}(x)$ (real and imaginary part) in domain. Table 1 shows a comparison of both the approximate $\hat{u}(x)$ and exact $u(x)$ solutions obtained from formula (21) for different number \bar{n} of expressions from the approximating sum (11).

Based on the relative error presented in Fig. 6 we see that the approximation of the function $\hat{u}(x)$ in domain polynomials of third degree ($\bar{n} = 9$) is exact if compared with analytical solutions. For testing the convergence of the method in the domain solution are approximated by the polynomials of the fourth degree ($\bar{n} = 16$). Obtained much more accurate results and shows the stability of the presented method.

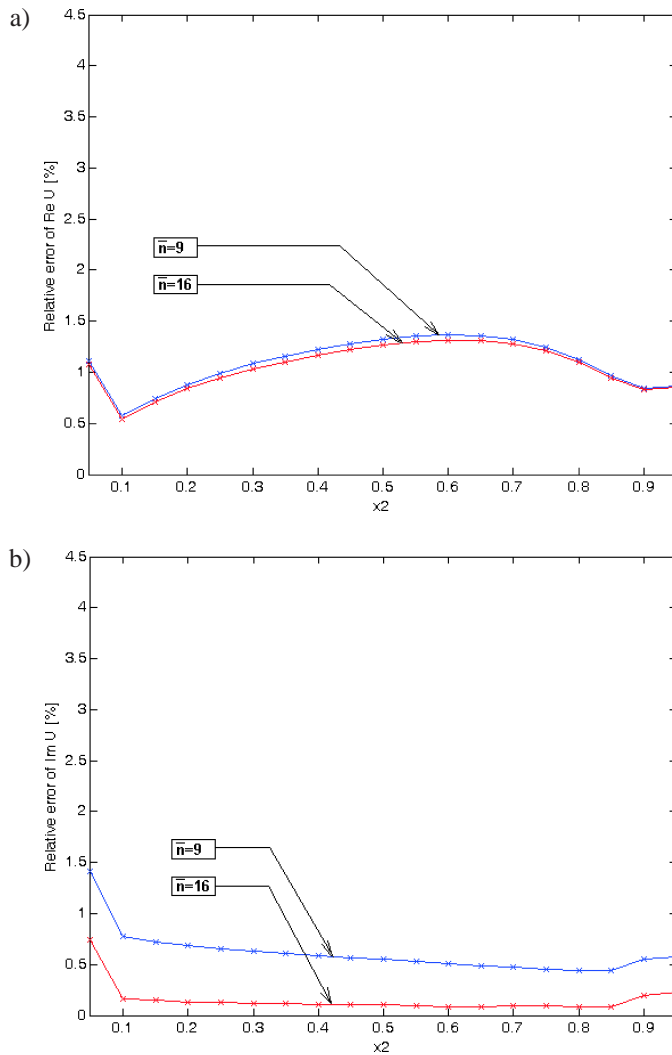


Fig. 6. Relative errors of solution in the domain obtained for different number of approximating series expressions ($\bar{n} = 9$ and $\bar{n} = 16$) from Table 1. a) real part, b) imaginary part.

To increase the accuracy of solutions in the PIES we only need to increase the number \bar{n} in the approximating series (11). From the programming point of view the operation simply involves changing the number in the program, which makes it possible to

Table 1. Comparison of solution in domain Ω ($k = 1$ and $\alpha = 30^\circ$) for different number of approximating series expressions. (The number of solved system of algebraic equations is given in parenthesis).

x_1	x_2	x_3	Analytical		Numerical			
			Re $u(x)$	Im $u(x)$	Re $\hat{u}(x)$	Im $\hat{u}(x)$	Re $\hat{u}(x)$	Im $u(x)$
					$\bar{n} = 9$ (eq. 108*)		$\bar{n} = 16$ (eq. 192*)	
1	2	3	4	5	6	7	8	9
0.25	0.1	0.5	1.464	0.263	1.473	0.265	1.472	0.263
0.25	0.2	0.5	1.450	0.311	1.463	0.313	1.462	0.311
0.25	0.3	0.5	1.433	0.358	1.449	0.360	1.448	0.358
0.25	0.4	0.5	1.414	0.404	1.431	0.406	1.431	0.405
0.25	0.5	0.5	1.393	0.449	1.411	0.452	1.410	0.450
0.25	0.6	0.5	1.369	0.536	1.388	0.496	1.387	0.494
0.25	0.7	0.5	1.343	0.352	1.361	0.539	1.361	0.537
0.25	0.8	0.5	1.315	0.578	1.330	0.580	1.330	0.578
0.25	0.9	0.5	1.285	0.618	1.296	0.621	1.296	0.619

* The number of solved system of algebraic equations is given in parenthesis.

quickly verify the convergence. This is a considerable advantage over the element methods in which the increase accuracy involves the increase of the number of elements.

7. Conclusions

The presented PIES method offers a new, more flexible way of solving the 3D Helmholtz equation. The separation of approximation of the boundary geometry from boundary functions in the PIES creates a new way in domain geometry definition and obtaining continuous solutions on boundary. Linear Coons surfaces used for boundary approximation provides a natural method to apply the domain and reduce the input data to a small set of corner points. A solution of PIES with proposed algorithm does not require the boundary discretization. Finally continuous solutions on each segment are obtained. The proposed method reduces the size of the system algebraic equations and the cost of computing. The testing examples confirm the accuracy and stability of the proposed algorithm.

References

- [1] ABRAMOWICZ A., STEGUN I., *Handbook of mathematical functions*, Dover, New York 1974.
- [2] AMINI S., KIRKUP M. S., *Solution of Helmholtz equation in the exterior domain by elementary boundary integral methods*, Journal of Computational Physics, **118**, 208–221 (1995).

-
- [3] AUTERI F., QUARTAPALLE L., *Galerkin-Legendere spectral method for the 3D Helmholtz equation*, Journal of Computational Physics, **161**, 454–483 (2000).
- [4] BREBBIA C. A., TELLES J. C. F., WROBEL L. C., *Boundary element techniques, theory and applications in engineering*, Springer, New York 1984.
- [5] CHEN J. T., *Recent development of dual BEM in acoustic problems*, Comput. Methods Appl. Mech. Eng., **188**, 833–845 (2000).
- [6] CISKOWSKI R. D., BREBBIA C. A., *Boundary element methods in acoustics*, Computational Mechanics, Southampton, Elsevier Applied Sciences, London 1991.
- [7] GEOTTLIEB D., ORSZAG S. A., *Numerical analysis of spectral methods*, SIAM, Philadelphia 1997.
- [8] HU F. Q., *A spectral boundary integral equation method for the 2D Helmholtz equation*, Journal of Computational Physics, **120**, 340–347 (1995).
- [9] KAMIYA N., ANDO E., NOGAE K., *A new complex-valued formulation and eigenvalue analysis of the Helmholtz equation by boundary element method*, Adv. Eng. Software, **26**, 219–227 (1996).
- [10] MORTENSON N. M., *Geometric modelling*, John and Sons, Chichester 1985.
- [11] POZRIKIDIS C., *A practical guide to Boundary-Element Methods with the software library BEMLIB*, Chapman & Hall/CRC Press, 2002.
- [12] RAVEENDRA S. T., *An efficient indirect boundary element technique for multi-frequency acoustic analysis*, Int. J. Numer. Meth. Engng., **44**, 59–76 (1999).
- [13] ZIENIUK E., *Bézier curves in the modification of boundary integral equations (BIE) for potential boundary-value problems*, International Journal of Solids and Structures, **40**, 9, 2301–2320 (2003).
- [14] ZIENIUK E., SZERSZEŃ K., BOŁTUĆ A., *Platy powierzchniowe Coonsa w modelowaniu trójwymiarowej geometrii brzegu w zagadnieniach brzegowych dla równania Laplace'a*, PTSK Symulacja w badaniach i rozwoju, 447–454, Kraków 2004.
- [15] ZIENIUK E., SZERSZEŃ K., BOŁTUĆ A., *Bézier and Coons surfaces in the modelling and modification of the 3-D potential boundary-values problems*, Computer Information Systems and Applications, vol. I, WSFiZ Press, 127–134, Białystok 2004.
- [16] ZIENIUK E., BOŁTUĆ A., *An algorithm for numerical solving of the two-dimensional Helmholtz equation using a parametric integral equations systems (PIES)*, [in:] Structures–Waves–Human Health, vol. XIII, No. 1, pp. 157–164 (2004).
- [17] ZIENIUK E., *Simple-layer potential with boundary modelling by B-spline curves for Helmholtz equations*, [in:] Structures–Waves–Biomedical Engineering, (X), 91–100, (2001).
- [18] ZIENIUK E., *Potential problems with polygonal boundaries by a BEM with parametric linear functions*, Engineering Analysis with Boundary Elements, **25**, 3, 185–190 (2001).
- [19] ZIENKIEWICZ O., *The Finite Element Methods*, McGraw-Hill, London 1977.